

EFFICIENT USE OF RARE EARTHS AS DOPANTS IN THE DEVELOPMENT OF ZrO_2 BASED MATERIALS

Anca Elena SLOBOZEANU¹, Radu Robert PITICESCU¹, Cristian PREDESCU²,
Ioan Albert TUDOR¹, Alexandru Cristian MATEI¹

Rare earth elements (REE) are among the most important materials used in high-tech components. An increasing interest has been observed in the use of various mixtures of rare earth oxides (REOs) as dopants for ceramic materials, especially for ZrO_2 . Rare earth elements are included in the list of critical materials by the EU, and for their extraction and separation from minerals, mining and processing techniques with high environmental impact are used.

This work aims to obtain ceramic materials based on zirconium doped with mixture of rare earth oxides (REO), with similar concentration ratios to that found in the mineral monazite, with an impact on the efficient consumption of rare earths and the production cost. Therefore, ZrO_2 doped with 8% Ln and Y_2O_3 (Ln= Ce, La, Nd, Gd) will be synthesized by hydrothermal synthesis technique. For the resulting material, the structure, morphology and thermal properties will be studied with a view to its potential use for applications in thermal barrier coatings (TBC).

Keywords: monazite, hydrothermal synthesis, ceramic materials, zirconia

1. Introduction

The monazite with generic formula $[(\text{REE})\text{PO}_4]$ is considered among the most valuable natural resources of oxides of rare earth elements (REE), elements that are widely used both for applications in traditional sectors such as: glass manufacturing [1][2] [3], metallurgy [4][5], agriculture [6][7], catalysis [8], but also for high-tech industries such as wind turbines [9] [10], e-mobility [11] [10][12], etc.

The term monazite, which originates from the Greek "monazein" meaning "to be solitary", comprises several groups named after the major cationic constituent: Monazite-(Ce) – (Ce, La, Nd, Th) (PO_4) , idealize CePO_4 ; Monazite - (La) – (La, Ce, Nd) (PO_4) , idealize LaPO_4 ; Monazite-(Nd) – (Nd, Ce, Sm) (PO_4) , idealize NdPO_4 ; Monazite - (Sm) – (Sm, Gd, Ce, Th) (PO_4) , idealize SmPO_4 . The color of the mineral can vary from yellow to brown or even red [13].

Separating individual REOs from monazite is a difficult process with a high

¹ Eng., National R&D Institute for Nonferrous and Rare Metals – IMNR, Pantelimon district, Bucharest Romania, corresponding author's e-mail: slobozeanu.anca@yahoo.com@yahoo.com

² Prof., Dept. of Ecometallurgy and Materials Processing, University POLITEHNICA of Bucharest, Romania

environmental impact and energy consumption reflected in high prices. This fact is due to the complexity of the process, the solvent extraction used requiring many steps of extraction and re-extraction, due to the fact that the REE have a very similar electronic configuration and physical-chemical properties [14] [15][16].

Various rare earth oxides (REOs) have recently been studied as dopants for new ZrO_2 -based thermal barrier coatings for various industrial applications [17] [18] [19] [20]. They have the role of improving the thermal conductivity and phase stability compared to the gold standard YSZ material (ZrO_2 doped with 8% Y). At present, 8YSZ is the most widely used thermal barrier material (TBC) due to its properties such as high fracture toughness, fast ionic conductivity and low thermal conductivity, usually in the range $1.8 - 3.0 \text{ W/mK}$ for $200 \text{ }^\circ\text{C} \leq T \leq 1000 \text{ }^\circ\text{C}$ [21]. However, the use of 8YSZ is limited at temperatures higher than $1200 \text{ }^\circ\text{C}$ due to the phase transformation of YSZ from the t' phase to the tetragonal (t) and cubic (c) phase, and then the t phase to the monoclinic (m) phase. For example, if Y is replaced by Yb an increase in phase stability is observed, but nevertheless the sintering resistance is reduced [22].

Several methods to obtain REO-doped ZrO_2 have been investigated: co-precipitation [23] [24], solid state reaction [25] [26], chemical precipitation [27]. This research aims at the potential use of naturally mixed REOs obtained directly from monazite concentrates as dopants in the field of high temperature ceramic materials.

The work focuses on the development by the hydrothermal method and the characterization of the ZrO_2 material doped with mixed REO, simulating the composition of selected monazite concentrates after removing the radioactive elements (Th, U and Ra), but also keeping elemental Ce. For this purpose, synthesis experiments were carried out using synthetic compositions of Ce-based rare earth anesthetics, studying the structure, morphology and thermal properties.

2. Materials and methods

2.1. Starting materials

The raw materials used were: $\text{Y}_2\text{O}_3 > 99\%$ -Merck, $\text{Nd}_2\text{O}_3 \geq 99,9\%$ -Alfa Aesar, $\text{Gd}_2\text{O}_3 \geq 99,9\%$ -Alfa Aesar și La $(\text{NO}_3)_3 \cdot 6\text{H}_2\text{O}$ - VWR Chemicals, Ce (III) $\text{N}_3\text{O}_9 \cdot 6\text{H}_2\text{O}$ – ACROS Organics- 99,5.

2.2. Hydrothermal synthesis

ZrO_2 powder doped with 8% mixed synthetic mixture of Ln (Ln = Ce, La, Nd, Gd) and Y_2O_3 , which is referred to below $\text{ZrO}_2\text{-CeRO}$ was obtained by hydrothermal process at moderate pressures (maximum 40 atm.) and moderate temperatures (maxim 250°C). The main advantages of this method are: one-step process, low energy consumption, use of low temperatures for crystallization, improved chemical reactivity, high homogeneity and control of nucleation and

growth [28] [29].

Preparation of aqueous Zr (IV) stock solution with programmed Zr concentration was made from zirconium tetrachloride (ZrCl_4 99% Merck) dissolved in distilled water and filtered to remove insoluble particles. In the solution thus obtained, the precursor was dissolved, under rigorous mechanical stirring. In order to obtain an alkaline suspension with a pH of approximately 9, the mineralizing agent, ammonia solution (NH_3 wt. 25 %, Chimreactiv srl), was added. The suspension thus obtained was hydrothermally treated (Berghoff, Germania, 5 L capacity, Berghoff Products + Instruments GmbH,) and cooled controlled with water using a coil inserted in the reaction vessel. Following the hydrothermal process, a solid precipitate was obtained, which was washed and filtered to remove soluble impurities, followed by oven drying at 110 °C until constant weight. The synthesis scheme is shown in the Fig.1.

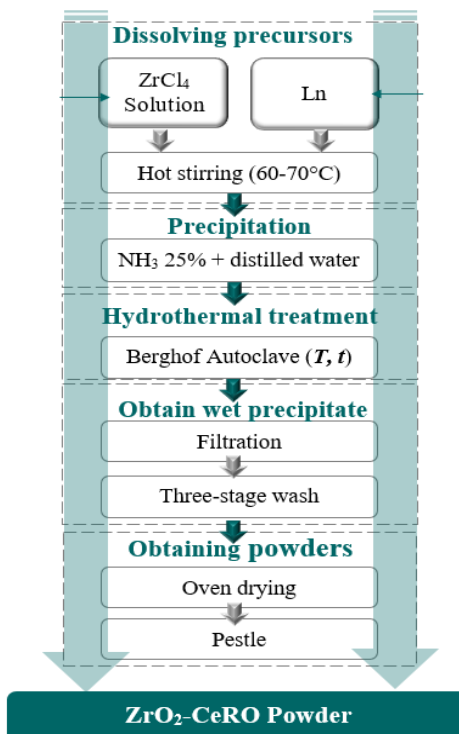


Fig. 1 Schematic representation of the hydrothermal synthesis process used to obtain ZrO_2 -CeRO powders.

2.2 Characterization methods

Chemical analysis of ZrO_2 -CeRO powder was performed by inductively coupled plasma optical emission spectrometry (Agilent 725 ICP-OES, Agilent Technologies Inc., Colorado Springs, CO, USA) according to ASTM E 1479-99

(2011).

The *microstructure* of the ZrO₂-CeRO powder was studied using a BRUKER D8 ADVANCE X-ray diffractometer (Bruker AXS GmbH, Karlsruhe, Germany) with monochromatic K α radiation, using the Bragg-Brentano diffraction method. To identify the phases contained in the sample, data processing was performed using the DIFFRAC.SUITE.EVA release 2016 software package by Bruker AXS, Karlsruhe, Germany; SLEVE + 2020 and the ICDD PDF-4 + 2020 database edited by the International Center for Diffraction Data (ICDD).

The sample *morphology* was investigated by scanning electron microscopy (SEM) using a Quanta 250 high resolution microscope (FEI Company, Eindhoven, The Netherlands) incorporated with the energy dispersive X-ray spectrometer manufactured by EDAX (Mahwah, NJ, USA), consisting of ELEMENT Silicon Drift Detector Fixed, Element EDS Analysis Software Suite APEX™ 1.0, EDAX, Mahwah, NJ, USA.

Thermal stability was analyzed by Differential scanning calorimetry coupled with thermal gravimetry analysis (DSC-TG) with a SETARAM SETSYS Evolution equipment (SETARAM Instrumentation, Caluire, France) under inert atmosphere. The samples were placed in alumina crucibles and heated at a heating rate of 10 K/min to 1450 °C, then cooled to room temperature at the same rate. Experimental data were processed using Calisto v.1.097 software (SETARAM Instrumentation, Caluire, France).

Thermal properties at room temperature were measured using the hot disk method (TPS 2200 Hot Disk, Hot Disk AB, Gothenburg, Sweden) on pairs of cylindrical pellets approximately 20 mm in diameter and 5 mm in height, heat treated at 1200 °C.

A Kapton sensor with a diameter of 2 mm (code 7577) was inserted between the two cylindrical samples. This was used to generate heat and monitor the temperature evolution of the sample. Thermal conductivity was calculated using data processing software developed by the manufacturer.

3. Results and discussion

3.1 Chemical analysis

Table 1 presents the chemical analysis of the ZrO₂-CeRO powder obtained by hydrothermal synthesis. This analysis confirms the designed composition. The concentration of Zr, Y and Ln in the mother liquor resulting from the filtration of the hydrothermal reaction products was <10⁻³ g·L⁻¹.

Table 1.

Chemical analysis for hydrothermally synthesized ZrO₂-CeRO powder.

Sample cod	Sample description	Unit	Ce	Gd [%]	La [%]	Nd [%]	Y [%]	Zr [%]
------------	--------------------	------	----	--------	--------	--------	-------	--------

ZrO_2 -CeRO	Powder obtained by hydrothermal synthesis	wt. %	1.52	0.14	0.93	1.57	0.14	67.8
S ZrO_2 -CeRO	The mother liquid resulting from the filtration of hydrothermal reaction products	g/l	<0.001	<0.001	<0.001	<0.001	<0.001	<0.001

3.2 XRD analysis

Fig.2 shows the X-ray diffraction (XRD) pattern of the ZrO_2 -CeRO powder synthesized by the hydrothermal method and dried at 110 °C, the quantitative phase analysis being presented in table 2.

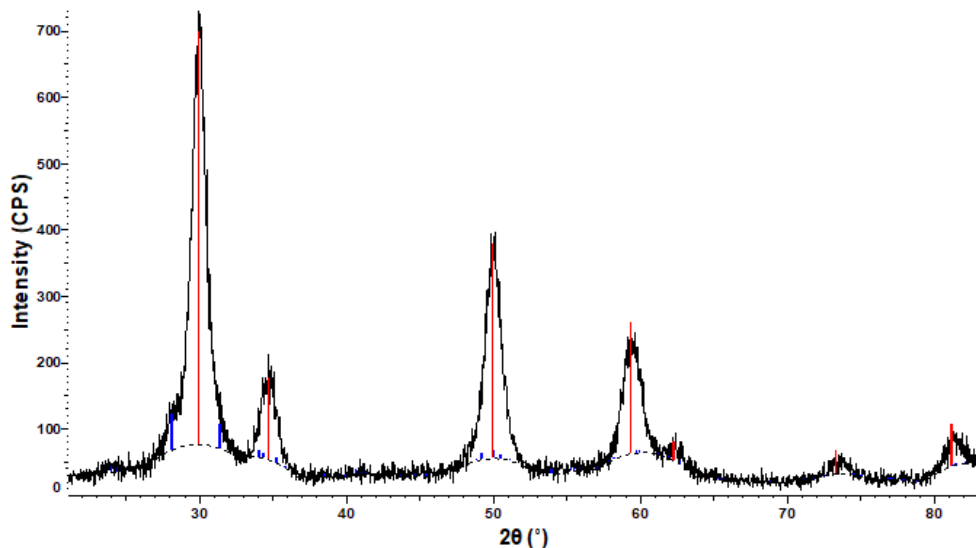


Fig. 2. X-ray diffraction of ZrO_2 -CeRO.

Table 1
Quantitative phase analysis of ZrO_2 -CeRO

Major phases		Formula	PDF File	Cristalization system
—	Baddeleyite	ZrO_2	PDF 04-015-4188	Monoclinic
—	Zirconium Yttrium Oxide type	Solid solution ZrO_2	PDF 01-084-2546	Cubic

The hydrothermally synthesized ZrO_2 -CeRO powder has cubic Yttrium Zirconium Oxide as the main phase and monoclinic (Baddeleyite) as the secondary

phase.

3.3 SEM analyzes

The SEM image shown in Fig.3 shows us that the ZrO_2 -CeRO powder consists of angular aggregates. The presence of elements and uniformly distributed in aggregates is also confirmed by EDS analysis.

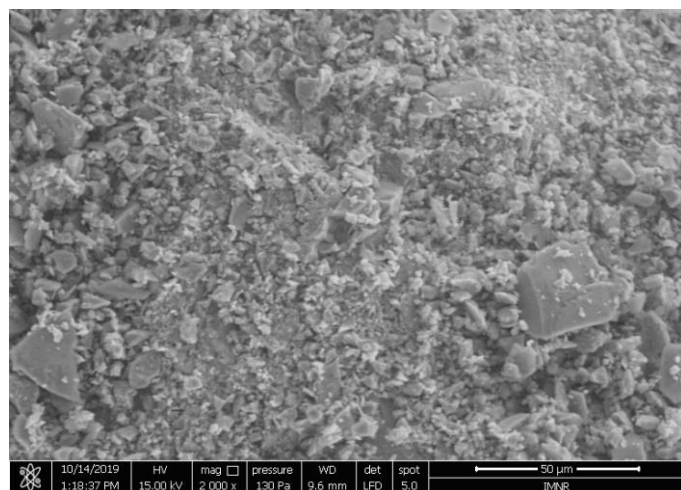


Fig. 3. SEM image of ZrO_2 -CeRO powder.

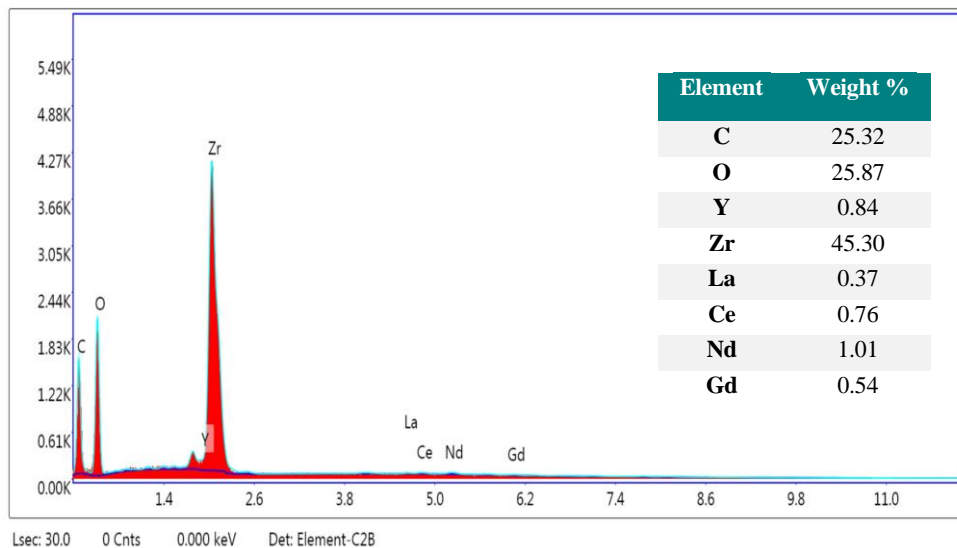


Fig. 4. EDS image of ZrO_2 -CeRO powder.

3.4 DCS-TG analyzes

In order to analyze the thermal stability and phase transformations during

the heat treatment of the hydrothermally obtained ZrO_2 -CeRO powder, thermal analysis was used.

The DSC-TG plot of ZrO_2 -CeRO powder heated from room temperature to 1450 °C is shown in the figure.

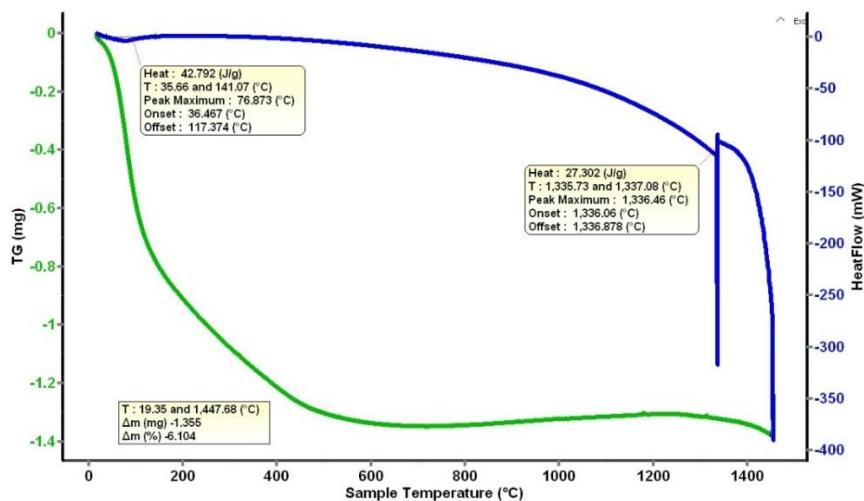


Fig. 5. DSC-TG analysis of ZrO_2 -CeRO powders.

The DSC-TG measurement shows a continuous mass loss up to 600 °C, and an endothermic peak around 76,97 °C, revealing a dehydration process of the ZrO_2 -CeRO material, which is in agreement with other studies of literature [30].

3.5 Thermal properties

Thermal conductivity is very important for the performance of materials in the TBC field. The thermal properties determined at room temperature of the ZrO_2 -CeRO material are presented in table 3.

Table 2
Thermal properties for ZrO_2 -CeRO powder.

Sample	Th. Conductivity (W/m·K)	Th. Diffusivity (mm ² /s)	Volumetric Spec. Heat (MJ/m ³ ·K)	Spec. Heat (MJ/m ³ ·K)
ZrO_2 -CeRO	0.6822 ± 0.0035	0.4118 ± 0.0167	1.6588 ± 0.0714	0.3806 ± 0.0164

The thermal conductivity values obtained on the ZrO_2 -CeRO powder are similar to those obtained in the work [31] where RE_2O_3 materials (RE = La, Yb, Ce and Gd) and ZrO_2 co-doped with Y_2O_3 was obtained by sol-gel methods. The thermal conductivities of RE-YSZ tetragonal powders (RE = La, Yb, Ce and Gd) were: 0,5181, 0,4215, 0,4851, 0,5187 and respectively 0,5347 W/mK.

4. Conclusion

Zirconium powder co-doped with 8 wt.% synthetic mixture of rare earth oxides was successfully synthesized by the hydrothermal method in a one-step process at moderate temperature (max. 250 °C) and pressures (max. .40 atm). A crystalline powder consisting of cubic Yttrium Zirconium Oxide as a single phase and monoclinic (Baddeleyite) as a secondary phase was obtained. The obtained thermal conductivity is similar to those obtained in other literature studies. These results confirm the potential use of REE mixtures as dopants for TBC applications, with impact on cost reduction and low environmental impact.

Acknowledgments

This work has been funded by: UEFISCDI in the frame of the Project ID PN-III-2.1-PED-2019-2175, “Modernized EB-PVD System for Development and Assessment of Thermal Barrier Coatings for Aeronautic Applications” AERO-COAT; ERANET-ERAMIN III “Recovery of Rare Earth Elements from complex concentrates from Turkey and their potential use in high-tech industrial applications” RETECH; and by European Social Found from the Sectoral Operational Programme Human Capital 2014-2020, throught the Financial Aggrement with the title “Training of PhD students and postdoctoral researchers skills – SMART” Contract no. 13530/16.06.2022- SMIS code: 153734.

R E F E R E N C E S

- [1] S. W. Yung *et al.*, “Thermal, chemical, optical properties and structure of Er³⁺-doped and Er³⁺/Yb³⁺-codoped P₂O₅–Al₂O₃–ZnO glasses,” *J. Non. Cryst. Solids*, vol. **357** (4,) 2011, pp. 1328–1334.
- [2] S. W. Yung *et al.*, “Concentration Effect of Yb³⁺ on the Thermal and Optical Properties of Er³⁺/Yb³⁺-codoped ZnF₂-Al₂O₃-P₂O₅ Glasses,” *Mater. Chem. Phys.*, vol. **117**(1), 2009, pp. 29–34.
- [3] Q. Shi *et al.*, “Effect of rare-earth oxides on structure and chemical resistance of calcium aluminophosphate glasses,” *J. Non. Cryst. Solids*, vol. **491**, 2018, pp. 71–78
- [4] A. Biesiekierski, Y. Li, and C. Wen, “The Application of the Rare Earths to Magnesium and Titanium Metallurgy in Australia,” *Adv. Mater.*, vol. **32**(18) May 2020, pp. 1901715.
- [5] F. Pan *et al.*, “Effects of Rare Earth Metals on Steel Microstructures,” *Materials* (Basel),, vol. **9**(6), May 2016.
- [6] F. Tommasi *et al.*, “Review of Rare Earth Elements as Fertilizers and Feed Additives: A Knowledge Gap Analysis,” *Arch. Environ. Contam. Toxicol.*, vol. **81**(4), Nov. 2021, pp. 531–540.
- [7] X. Pang, D. Li, and A. Peng, “Application of rare-earth elements in the agriculture of china and its environmental behavior in soil,” *J. Soils Sediments*, vol. **1**(2) Jun. 2001, pp. 124–129.
- [8] J. Feng, X. Zhang, J. Wang, X. Ju, L. Liu, and P. Chen, “Applications of rare earth oxides in catalytic ammonia synthesis and decomposition,” *Catal. Sci. Technol.*, vol. **11**(19), Oct. 2021, pp. 6330–6343.

- [9] *S. Verma, A. R. Paul, and N. Haque*, “Assessment of Materials and Rare Earth Metals Demand for Sustainable Wind Energy Growth in India,” *Minerals*, vol. **12**(5), 2022, p. 647.
- [10] *P. Alves Dias, S. Bobba, S. Carrara, and B. Pazzotta*, The role of rare earth elements in wind energy and electric mobility. 2020.
- [11] *M. Anenburg, J. A. Mavrogenes, C. Frigo, and F. Wall*, “Rare earth element mobility in and around carbonatites controlled by sodium, potassium, and silica,” *Sci. Adv.*, vol. **6**(41), Oct. 2020.
- [12] *D. Gielen and M. Lyons*, Critical materials for the energy transition: Rare earth elements. 2022.
- [13] *B. Schulz*, “Monazite Microstructures and Their Interpretation in Petrochronology,” *Front. Earth Sci.*, vol. **9**, Apr. 2021,
- [14] *J. Zhang, B. Zhao, and B. Schreiner*, “Separation hydrometallurgy of rare earth elements,” *Sep. Hydrometall. Rare Earth Elem.*, Feb. 2016, pp. 1–259.
- [15] *D. Kołodyńska, D. Fila, B. Gajda, J. Gęga, and Z. Hubicki*, “Rare Earth Elements—Separation Methods Yesterday and Today,” *Appl. Ion Exch. Mater. Environ.*, **2019**, pp. 161–185.
- [16] *F. Xie, T. A. Zhang, D. Dreisinger, and F. Doyle*, “A critical review on solvent extraction of rare earths from aqueous solutions,” *Miner. Eng.*, vol. **56**, 2014, pp. 10–28.
- [17] *Y. Ozgurluk, K. M. Doleker, and A. C. Karaoglanli*, “Hot corrosion behavior of YSZ , $\text{Gd}_2\text{Zr}_2\text{O}_7$ and $\text{YSZ}/\text{Gd}_2\text{Zr}_2\text{O}_7$ thermal barrier coatings exposed to molten sulfate and vanadate salt,” *Appl. Surf. Sci.*, vol. **438**, Apr. 2018, pp. 96–113.
- [18] *L. Yang et al.*, “Investigation of mechanical and thermal properties of rare earth pyrochlore oxides by first-principles calculations,” *J. Am. Ceram. Soc.*, vol. **102**(5) May 2019, pp. 2830–2840.
- [19] *Z. Chen*, “Global rare earth resources and scenarios of future rare earth industry,” *J. Rare Earths*, vol. **29**(1), Jan. 2011, pp. 1–6.
- [20] *K. M. Goodenough et al.*, “Europe’s rare earth element resource potential: An overview of REE metallogenetic provinces and their geodynamic setting,” *Ore Geol. Rev.*, vol. **72**, Jan. 2016, pp. 838–856.
- [21] *R. J. Takahashi, J. M. K. Assis, F. Piorino Neto, and D. A. P. Reis*, “Thermal conductivity study of $\text{ZrO}_2\text{-YO1.5-NbO2.5 TBC}$,” *J. Mater. Res. Technol.*, vol. **19**, Jul. 2022, pp. 4932–4938.
- [22] *K. Jiang, S. Liu, Y. Li, and Y. Li*, “Effects of RE^{3+} Ionic Radius on Monoclinic Phase Content of 8 mol% REO1.5 Partially Stabilized ZrO_2 ($\text{RE} = \text{Yb, Y, Gd, and Nd}$) Powder Compacts after Annealing at High Temperature,” *J. Am. Ceram. Soc.*, vol. **97**(3), Mar. 2014, pp. 990–995.
- [23] *R. Mekala, B. Deepa, and V. Rajendran*, “Preparation, characterization and antibacterial property of rare earth (Dy and Ce) doping on ZrO_2 nanoparticles prepared by co-precipitation method,” *Mater. Today Proc.*, vol. **5**(2), Jan. 2018, pp. 8837–8843.
- [24] *C. Chen et al.*, “Effect of scandia content on the hot corrosion behavior of Sc_2O_3 and Y_2O_3 co-doped ZrO_2 in $\text{Na}_2\text{SO}_4 + \text{V}_2\text{O}_5$ molten salts at 1000 °C,” *Corros. Sci.*, vol. **158**, Sep. 2019, pp. 108094.
- [25] *X. Song, M. Xie, R. Mu, F. Zhou, G. Jia, and S. An*, “Influence of the partial substitution of Y_2O_3 with Ln_2O_3 ($\text{Ln} = \text{Nd, Sm, Gd}$) on the phase structure and thermophysical properties of $\text{ZrO}_2\text{-Nb}_2\text{O}_5\text{-Y}_2\text{O}_3$ ceramics,” *Acta Mater.*, vol. **59**(10), Jun. 2011, pp. 3895–3902.
- [26] *Y. T. Wang, L. Chen, and J. Feng*, “Impact of ZrO_2 alloying on thermo-mechanical properties of $\text{Gd}_3\text{Nb}_7\text{O}_7$,” *Ceram. Int.*, vol. **46**(5), Apr. 2020, pp. 6174–6181.
- [27] *M. Bahamirian, S. M. M. Hadavi, M. Farvizi, M. R. Rahimipour, and A. Keyvani*, “Phase stability of $\text{ZrO}_2\text{ 9.5Y}_2\text{O}_3\text{ 5.6Yb}_2\text{O}_3\text{ 5.2Gd}_2\text{O}_3$ compound at 1100 °C and 1300 °C for advanced TBC applications,” *Ceram. Int.*, vol. **45**(6) Apr. 2019, pp. 7344–7350.

- [28] “Handbook of Hydrothermal Technology - K. Byrappa, Masahiro Yoshimura - Google Cărți.” https://books.google.ro/books?hl=ro&lr=&id=vA5tXzLsHioC&oi=fnd&pg=PP1&ots=cyqa bYhnhk&sig=Qq8IDpzomLqyQT6JOf0HN4WGJcQ&redir_esc=y#v=onepage&q&f=false (accessed Aug. 19, 2022).
- [29] *S. Machmudah et al.*, “Synthesis of ZrO₂ nanoparticles by hydrothermal treatment,” AIP Conf. Proc., vol. **1586**, February 2015, pp. 166–172,
- [30] *C. Hennig, S. Weiss, R. Gumeniuk, and A. C. Scheinost*, “Phase composition of yttrium-doped zirconia ceramics,” Institute of Resource Ecology, Annual Report, 2016.
- [31] *Q. Shi, W. Yuan, X. Chao, and Z. Zhu*, “Phase stability, thermal conductivity and crystal growth behavior of RE₂O₃ (RE = La, Yb, Ce, Gd) co-doped Y₂O₃ stabilized ZrO₂ powder,” *J. Sol-Gel Sci. Technol.*, vol. **84**(2), 2017, pp. 341–348.